Effect of Bidentate Ligand Additive in Tin Perovskite Solar Cells

Dhruba B. Khadka[1], Yasuhiro Shirai[1], Masatoshi Yanagida[1] and Kenjiro Miyano[1]

[1]Photovoltaics Materials Group, Global Research Center for Environment and Energy based on Nanomaterials Science (GREEN), National Institute for Materials Science (NIMS), 1-1 Namiki, Tsukuba, Ibaraki 305-0044, Japan

***Abstract* — Tin- perovskite solar cell (Sn-PSC) is limited by their poor stability arising from facile tin oxidation and uncontrolled film growth. Here, we introduced a multifunctional bidentate ligand, formohydrazide (FHZ) as an additive into $FASnI_3$ perovskite film. This additive is found to be effective for the control of Sn-oxidation and forms pin-hole free film morphology. The Sn-PSCs with FHZ additive enhanced the device efficiency from 9.93% (for control Sn-HaP) to 13.14 % (for device with FHZ additive) with higher reproducibility and superior device stability. The device analysis suggests that the hydrazide additive significantly passivates the bulk and surface defect in the Sn-PSCs. This report gives insights into the film growth properties, device photo-physics, and defect analysis correlating with device performance and device stability.**

I. INTRODUCTION

Lead perovskite solar cells (Pb-PSCs) have scaled up their power conversion efficiency (PCE) >25% in the past decade.[1], [2] But the toxic Pb has imposed a hurdle in commercialization due to health hazards. Therefore, lead-free perovskite candidates have centred colossal attention on replacing Pb.[3]–[6] Among the various alternative candidates, tin perovskite (Sn-HaP) derivates are excellent candidates with ideal bandgaps of 1.2- 14 eV.[7] It is reported that the intrinsic instability is due to the facile oxidation of Sn^{2+}, poor film growth, and shorter carrier lifetime.[8]

Several reports have been documented on reducing Sn^{2+} oxidation, surface passivation, structural regulation, and bulk or interface engineering, for the improvement in PCE as well as device stability in the Sn-PSCs.[9]–[12] Ning and co-workers have documented well-controlled crystal orientation using precursors SnI_2 adduct comprised with PEABr.[13] A PCE of 14.81% has been reported by modulating the 2D/3D microstructures using fluorine functionalized F-PEABr.[11] Indeed, functional additives engineering is effective in attuning the growth of the highly orientated crystalline film, defect attenuation, and carrier transport.

In this report, we used a bidentate ligand, formohydrazide (FHZ) as an additive in the Sn-HaP precursor solution to control the oxidation and film growth. The PCE of FHZ added device enhanced from 9.93 to 13.14 % with superior device stability. It is found that the FHZ additive results in high-quality Sn-HaP film with highly oriented crystalline growth, well-compact film texture, and control of the extent of Sn^{2+} oxidation. This work underscores a detailed insight into the effect of bidentate ligand in Sn-PSCs.

II. EXPERIMENTAL

A. Device fabrication

For the fabrication of $FASnI_3$; Sn-based HaP precursor solution (0.85 M) was prepared by dissolving a 0.92:0.08:10:1 stoichiometric ratio of FAI, RbCl, SnI_2, and SnF2 adding EDAI-0.01 M and PEABr-0.05 M in dimethyl sulfoxide (DMSO) solvent. For FHZ additive precursor, FHZ at a molar ratio of 2, 4, 8, 12, 16, 20, and 30% to SnI_2 was added to the above solution. The Sn-HaP precursor was deposited on the PEDOT:PSS (30 nm)/ITO substrate. These films were annealed on the hot plate at 60 ℃ for 1min and 850 ℃ for 10 min. Then, the device is completed depositing PCBM /BCP thin films were spun-coated on top of the Sn-HaP films. Finally, Ag (100 nm) was thermally evaporated and get device. The detailed fabrication can be found in our earlier report.[14]–[16]

B. Materials and device characterizations

The XRD results were collected using Rigaku Smart Lab, CuKα radiation, λ=1.5405Å. The SEM images were obtained by a high-resolution scanning electron microscope (SEM) at 5 kV accelerating voltage (Hitachi, S-4800). XPS spectra were obtained using a Versa Probe II (ULVAC-PHI, Japan). The current density–voltage (J-V) curves were measured under 1 sun with an AM1.5G spectral filter (100 mW/cm^2) coupled with an MPPT system (Systemhouse Sunrise Corp.). capacitance spectra (C–f) were collected using an LCR meter (IM3536, Hioki) under dark.

III. RESULTS AND DISCUSSION

The Sn-HaP films were fabricated by spin-coating precursor solution with FHZ, bidentate ligand for the improvement in the crystallization and passivating defect chemistry in the film.

To evaluate the effect of the FHZ additive on the photovoltaic performance, we fabricated Sn-PSCs with the inverted device architectures of ITO/PEDOT:PSS/Sn-HaP/ICBA/BCP/Ag as shown in the cross-sectional image (Fig. 1). The density-voltage (J-V) characteristics with varying FHZ contents are given in Fig. 1b. The statistical data (Fig. 1c) show theb trend of device efficiency with varying FHZ additive contentration. It demonstrated the best device with FHZ additive (12 mol%). The control device achieved a PCE of 9.93% (with J_{SC} ~19.62

mA/cm^2, V_{OC} ~0.734 V, and FF ~69.01%). The device with FHZ additive (≤12 mol%) in Sn-HaP (hereafter, Sn-PSC with FHZ) improved the device PCE of ~13.14% with a significant increase in V_{OC} ~0.892 V and FF ~75.2%.

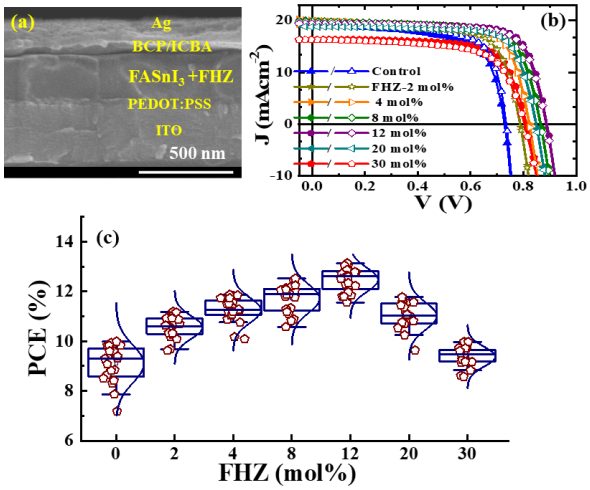

Fig. 1. Cross-sectional image of the device (a). The J-V curves of FAPSnI3+FHZ additive (for x=0 – 30 mol%) (b). Device efficiency trend with content of FHZ additive.

X-ray diffraction (XRD) patterns of Sn-HaP films with FHZ additive (selective mol%) are shown in Fig. 2a. XRD patterns reveal the characteristic diffraction assigned to highly oriented crystallographic planes of (100) and (200) which can be assigned to the orthorhombic phase of $FASnI_3$.[9,35] There is no shifting of characteristics XRD peak for the control or FHZ-added Sn-HaP films suggesting not incorporated in the Sn-HaP crystal lattice. The Sn-HaP film with FHZ additive (20 mol%) showed comparatively intensified XRD characteristic peaks indicating improved crystallinity. This is parallel to the trend of device performance.

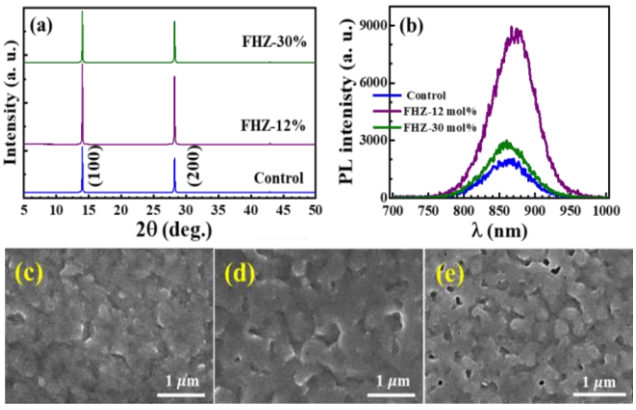

Fig. 2. Effect of FHZ additiveon; XRD patterns (a), PL spectra (b), and SEM images of Sn-HaP film FHZ additives.

Figure 2b depicts the PL spectra of corresponding films. The Sn-HaP film with the FHZ additive shows a higher peak intensity compared to the control film indicating ameliorated film quality with the FHZ additive. This observation is also consistent with the XRD peak intensity. The characteristic PL peaks are found to be centred at 1.430 ± 0.02 eV for the control and 1.416 ± 0.02 eV for 12 mol% FHZ.

Figure 2c-e depicts scanning electron microscopic images of the control and FHZ additive films. The films with FHZ additive show compact and better film coverage by suppressing the pinhole's densities. Small granular features in the control film disappeare in the FHZ-added Sn-HaP film. However, the Sn-HaP with a higher FHZ additive (30 mol%) was found to grow with pinholes and uneven morphology.

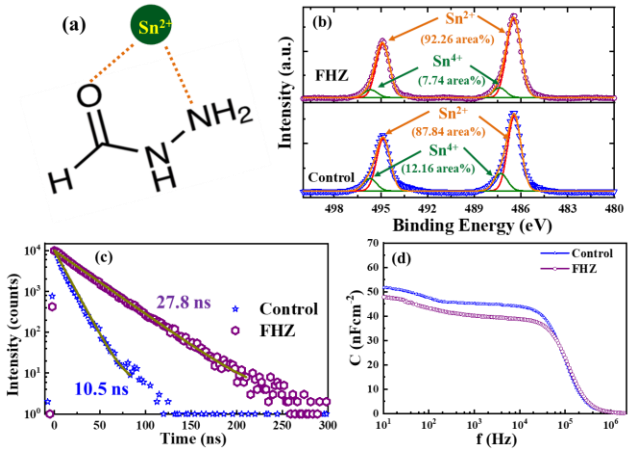

Fig. 3. XPS spectra (S-2p, Sn-3d) of the respective film (a,b). TRPL results of films (c). C-f spectra at room temperature (d).

Figure 3a shows the shematics of bonding interation of FHZ additive to the Sn-sites in Sn-perovskite. The FHZ additive strongly binds the Sn^{2+} molecules via -NH_2 and -O=C bidentate ligand which control the extent of Sn^{2+} oxidation.

Figure 3b presents the two characteristic peaks deconvoluted into the Sn 3d (3d5/2 (3d3/2)) at ~486.7 (495.2) eV and 487.3 (495.7) eV which are attributed to the Sn^{2+} and Sn^{4+} species, respectively. The Sn-HaP film shows suppression of the ionic percentage of Sn^{4+} from 12.16 to 7.74%. It corporates that FHZ can act as a bidentate ligand with metal. It forms a coordination complex with Sn^{2+} which control the formation of deleterious chemical derivatives such as Sn^{4+}.

Figure 3c shows the time-resolved photoluminescence (TRPL). The FHZ-treated HaP film demonstrated a longer carrier lifetime (τ-1~27.8 ns) compared to the control film (τ-~10.5 ns) suggesting suppression of the recombination pathways in the Sn-HaP film with FHZ additive. Hence, it leads to improvement in device performance.

Moreover, Fig. 3d shows the capacitance-frequency (C-f) spectra of the control and FHZ additive devices. Note that the capacitance at a lower frequency accounts for the ionic motion or charge accumulation.[17] The device with the FHZ additive

has a lower value indicating the reduction in ion or charge accumulation at the interfacial layer or electrode. While the control device reveals a slightly larger value in the frequency range of 1kHz < f < 50 kHz, which indicates a higher defect density in the control Sn-HaP film. It is concurrent with the device results.

IV. SUMMARY AND CONCLUSIONS

We have achieved the Sn-PSC of efficiency ~13.14 % using formohydrazide additive (9.93 % for the control device) with superior stability. The $FASnI_3$ film with the FHZ additive not only improved the film morphology and highly oriented crystal growth but also inhibited Sn^{2+}/Sn^{4+} oxidation benefiting from bidentate legend. The $FASnI_3$ film with FHZ additive increases the carrier lifetime suggesting the suppression of defect densities in the bulk and at the interface as supported capacitance spectra. This report substantiates that the antioxidative functional additive is expedient for the control of oxidation and defect passivation which scales up for the performance and stability of Sn-PSCs.

ACKNOWLEDGMENT

This work was supported by JST-Mirai Program Grant Number JPMJMI21E6, Japan.

REFERENCES

[1] O. Almora *et al.*, "Device Performance of Emerging Photovoltaic Materials (Version 3)," *Adv. Energy Mater.*, vol. 13, no. 1, p. 2203313, Jan. 2023, doi: 10.1002/aenm.202203313.

[2] D. B. Khadka, Y. Shirai, M. Yanagida, T. Tadano, and K. Miyano, "Interfacial Embedding for High-Efficiency and Stable Methylammonium-Free Perovskite Solar Cells with Fluoroarene Hydrazine," *Adv. Energy Mater.*, vol. 12, no. 38, p. 2202029, Oct. 2022, doi: 10.1002/aenm.202202029.

[3] M. G. M. Pandian *et al.*, "Effect of solvent vapour annealing on bismuth triiodide film for photovoltaic applications and its optoelectronic properties," *J. Mater. Chem. C*, vol. 8, no. 35, pp. 12173–12180, 2020, doi: 10.1039/D0TC02455D.

[4] G. Nasti and A. Abate, "Tin Halide Perovskite (ASnX3) Solar Cells: A Comprehensive Guide toward the Highest Power Conversion Efficiency," *Adv. Energy Mater.*, vol. 10, no. 13, p. 1902467, Apr. 2020, doi: 10.1002/aenm.201902467.

[5] S. T. Umedov, D. B. Khadka, M. Yanagida, A. Grigorieva, and Y. Shirai, "A-site tailoring in the vacancy-ordered double perovskite semiconductor Cs2SnI6 for photovoltaic application," *Sol. Energy Mater. Sol. Cells*, vol. 230, p. 111180, Sep. 2021, doi: 10.1016/j.solmat.2021.111180.

[6] D. B. Khadka, Y. Shirai, M. Yanagida, and K. Miyano, "Tailoring the film morphology and interface band offset of caesium bismuth iodide-based Pb-free perovskite solar cells," *J. Mater. Chem. C*, vol. 7, no. 27, pp. 8335–8343, 2019, doi: 10.1039/C9TC02181G.

[7] M. Baranowski and P. Plochocka, "Excitons in Metal-Halide Perovskites," *Adv. Energy Mater.*, vol. 10, no. 26, p. 1903659, Jul. 2020, doi: 10.1002/aenm.201903659.

[8] X. Liu *et al.*, "Templated growth of FASnI 3 crystals for efficient tin perovskite solar cells," *Energy Environ. Sci.*, vol. 13, no. 9, pp. 2896–2902, 2020, doi: 10.1039/D0EE01845G.

[9] M. A. Kamarudin *et al.*, "Suppression of Charge Carrier Recombination in Lead-Free Tin Halide Perovskite via Lewis Base Post-treatment," *J. Phys. Chem. Lett.*, vol. 10, no. 17, pp. 5277–5283, Sep. 2019, doi: 10.1021/acs.jpclett.9b02024.

[10] D. B. Khadka, Y. Shirai, M. Yanagida, and K. Miyano, "Attenuating the defect activities with a rubidium additive for efficient and stable Sn-based halide perovskite solar cells," *J. Mater. Chem. C*, vol. 8, no. 7, pp. 2307–2313, 2020, doi: 10.1039/C9TC06206H.

[11] B. Bin Yu *et al.*, "Heterogeneous 2D/3D Tin-Halides Perovskite Solar Cells with Certified Conversion Efficiency Breaking 14%," *Adv. Mater.*, vol. 33, no. 36, p. 2102055, Sep. 2021, doi: 10.1002/adma.202102055.

[12] D. B. Khadka, Y. Shirai, M. Yanagida, and K. Miyano, "Passivation of the Recombination Activities with Rubidium incorporation for Efficient and Stable Sn- HaP Solar Cells," in *2020 47th IEEE Photovoltaic Specialists Conference (PVSC)*, 2020, pp. 0113–0116, doi: 10.1109/PVSC45281.2020.9300783.

[13] X. Jiang *et al.*, "One-Step Synthesis of SnI2·(DMSO)x Adducts for High-Performance Tin Perovskite Solar Cells," *J. Am. Chem. Soc.*, vol. 143, no. 29, pp. 10970–10976, Jul. 2021, doi: 10.1021/jacs.1c03032.

[14] D. B. Khadka, Y. Shirai, M. Yanagida, and K. Miyano, "Pseudohalide Functional Additives in Tin Halide Perovskite for Efficient and Stable Pb-Free Perovskite Solar Cells," *ACS Appl. Energy Mater.*, vol. 4, no. 11, pp. 12819–12826, Nov. 2021, doi: 10.1021/acsaem.1c02496.

[15] D. B. Khadka, Y. Shirai, M. Yanagida, and K. Miyano, "Effect of Phenethylammonium Thiocyanate Additive in Tin Perovskite for Efficient and Stable Pb-free Perovskite Solar Cells," in *2022 IEEE 49th Photovoltaics Specialists Conference (PVSC)*, 2022, pp. 0004–0006, doi: 10.1109/PVSC48317.2022.9938869.

[16] D. B. Khadka, Y. Shirai, M. Yanagida, T. Masuda, and K. Miyano, "Enhancement in efficiency and optoelectronic quality of perovskite thin films annealed in MACl vapor," *Sustain. Energy Fuels*, vol. 1, no. 4, pp. 755–766, 2017, doi: 10.1039/C7SE00033B.

[17] D. B. Khadka, Y. Shirai, M. Yanagida, and K. Miyano, "Insights into Accelerated Degradation of Perovskite Solar Cells under Continuous Illumination Driven by Thermal Stress and Interfacial Junction," *ACS Appl. Energy Mater.*, vol. 4, no. 10, pp. 11121–11132, Oct. 2021, doi: 10.1021/acsaem.1c02037.